DOI: 10.1111/jbi.13101

ORIGINAL ARTICLE

WILEY Journal of Biogeography

Ancient mitochondrial genomes reveal the demographic history and phylogeography of the extinct, enigmatic thylacine (*Thylacinus cynocephalus*)

Lauren C. White[1,2] | Kieren J. Mitchell[1] | Jeremy J. Austin[1]

[1]Australian Centre for Ancient DNA, School of Biological Sciences, University of Adelaide, Adelaide, SA, Australia

[2]Department of Primatology, Max Planck Institute for Evolutionary Anthropology, Leipzig, Saxony, Germany

Correspondence
Jeremy J Austin, Australian Centre for Ancient DNA, School of Biological Sciences, University of Adelaide, Adelaide, SA, Australia.
Email: jeremy.austin@adelaide.edu.au

Funding information
ARC Future Fellowship, Grant/Award Number: FT10010008; Discovery Project, Grant/Award Number: DP130104055

Editor: Alexandre Antonelli

Abstract

Aim: The Tasmanian tiger, or thylacine, is an infamous example of a recent human-mediated extinction. Confined to the island of Tasmania in historical times, thylacines were hunted to extinction <150 years after European arrival. Thylacines were also once widespread across the Australian mainland, but became extinct there *c.* 3,200 years before present (BP). Very little is known about thylacine biology and population history; the cause of the thylacines extirpation from the mainland is still debated and the reasons for its survival in Tasmania into the 20th century are unclear. In this study, we investigate the thylacine's phylogeography and demographic history leading up to their extinction on both the mainland and Tasmania to gain insight into this enigmatic species.

Location: Southern Australia.

Methods: We generated 51 new thylacine mitochondrial DNA (mtDNA) genome sequences from sub-fossil remains and historical museum specimens, and analysed them to reconstruct the species' phylogeography and demographic history.

Results: We found evidence that thylacines had contracted into separate eastern and western populations prior to the Last Glacial Maximum (*c.* 25,000 yr BP), and that the ancient western population was larger and more genetically diverse than the historical Tasmanian population. At the time of European arrival in *c.* 1800 CE, Tasmanian thylacines had limited mtDNA diversity, possibly resulting from a bottleneck event broadly coincident with an El Niño-Southern Oscillation (ENSO) associated climate event, although we find some indication that the population was expanding during the late Holocene.

Main Conclusions: The timing of this putative expansion, in concert with a climate event, suggests that climate change had an influence on thylacine population dynamics. Given that ENSO effects are known to have been more severe on mainland Australia, we suggest that climate change, in synergy with other drivers, is likely to have contributed to the thylacine mainland extinction.

KEYWORDS
aDNA, ancient DNA, Australia, extinction, mitogenomes, phylogenetics, phylogeography, Tasmanian tiger, Tasmanian wolf

1 | INTRODUCTION

The Tasmanian tiger, or thylacine (*Thylacinus cynocephalus*; Harris, 1808), was a marsupial carnivore infamous for its recent, human-mediated extinction. At the time of European arrival in Australia in the late 1700s, the species was found only in Tasmania. It became extinct <150 years later, likely due to hunting encouraged by bounty schemes initiated because of its perceived impact on introduced livestock (Owen, 2003). The Tasmanian devil (*Sarcophilus harrisii*), similarly confined to Tasmania, then inherited the title of the largest extant marsupial carnivore. Both species were also once widespread across mainland Australia before declining to extinction there approximately 3,200 years before present (BP; Johnson, 2006).

The driver(s) of the late-Holocene mainland extinctions is still debated. Changes in climate, human intensification (i.e. development of advanced tools and population size increase), and the introduction of the dingo are the three main hypothesized causes (Prowse, Johnson, Bradshaw & Brook, 2013). The basis for these hypotheses is the timing of the changes/events and the isolation of Tasmania from their likely impacts. For example, the dingo (*Canis lupus dingo*)—a potential predator and competitor of the thylacine and devil—was introduced to mainland Australia *c.* 5,000 yr BP but never reached Tasmania as rising sea levels had flooded Bass Strait thousands of years earlier (*c.* 14,000 yr BP; Corbett, 1995). Similarly, human population size and hunting impacts increased on mainland Australia during the Holocene while this trend was markedly absent in Tasmania, where population size remained low (Johnson & Wroe, 2003). Finally, following the relatively wet and stable period of the Holocene optimum (*c.* 8,000–5,000 yr BP), a strengthening of the El Niño Southern Oscillation (ENSO) caused a shift in Australia's climate towards a drier, more drought-prone system (Donders, Wagner-Cremer & Visscher, 2008).

The effects of late-Holocene ENSO activity are assumed to have had a lesser influence on Tasmania—due to its maritime climate and more consistent rainfall (Donders, Haberle, Hope, Wagner & Visscher, 2007; Donders et al., 2008; Rees, Cwynar & Fletcher, 2015) and hence, had a reduced impact on Tasmanian devils and thylacines (Brown, 2006). However, a recent genetic study found evidence for a bottleneck in the Tasmanian devil population that is coincident with a peak in ENSO activity and the mainland population's extinction approximately 3,200 yr BP (Brüniche-Olsen, Jones, Austin, Burridge & Holland, 2014). The absence of other possible drivers in Tasmania suggests that shifts in climate may have initiated the decline of devil populations in Tasmania and the mainland. The combined pressure of climate change, dingoes and/or human intensification on the mainland may have led to the devil's extinction there. Given that climate change effects are expected to have been greater on the mainland than on Tasmania, Brüniche-Olsen et al. (2014) suggest that climate change may have been underestimated as a driver of the late-Holocene extinctions.

The late-Holocene bottleneck in Tasmanian devils resulted in the observed low genetic diversity in the population today (Jones, Paetkau, Geffen & Moritz, 2004). Similar patterns have been observed in historic Tasmanian thylacines (Menzies et al., 2012), suggesting a common population history in the two species. However, due to the rapidity of the decline of thylacines we know very little about their biology and population history. Additionally, lack of temporal sampling has thus far prohibited analyses of historical demography and range-wide phylogeographic structure in thylacines. We obtained 51 new thylacine mitochondrial genome sequences, including the first sequences from ancient samples from both Tasmania and the mainland. We used these data to investigate the demographic history of thylacines and test the hypothesis that they underwent a similar population decline to the Tasmanian devils during the late-Holocene.

2 | MATERIALS AND METHODS

2.1 | Sample collection, DNA extraction and radiocarbon dating

We collected <2 g of bone, tooth or dried tissue from 81 mainland and Tasmanian thylacines held in various museums (Figure 1, also see Appendix S1, Table S1.1 in supporting information) using a Dremel tool (Racine, WI, USA) fitted with Dremel cut-off wheel #409 (for bone samples) or sterilised scalpel blades (for tissue samples).

We controlled for contamination of the subfossil and historic museum samples with contemporary DNA by conducting all pre–PCR work in a dedicated and physically separate clean–room DNA facility at the Australian Centre for Ancient DNA, University of Adelaide. Laboratory protocols followed standard ancient DNA workflows to minimize contamination (Appendix S2).

DNA extraction was performed using the protocol described in Brotherton et al. (2013) with some modifications (see Appendix S2). Subfossil samples with enough material left after DNA extraction (n = 19) were submitted for radiocarbon dating at the Australian National University or the University of Waikato. We calibrated all ^{14}C dates to calendar years (BP) using the Southern Hemisphere Calibration curve (ShCal13) from the OxCal radiocarbon calibration tool Version 4.2 (https://c14.arch.ox.ac.uk). Historical museum samples without a known collection date (n = 15) were assigned an age of 120 yr BP as an intermediate age between the death of the last known thylacine in 1936 and establishment of the Tasmanian Museum and Art Gallery in 1843, from which many of the historic samples were sourced. We define ancient samples as those that are >600 years old and historical samples as those that are <600 years old or that were recently deceased at the time of collection if no date was recorded.

2.2 | Library preparation and hybridization enrichment

We built double-stranded Illumina libraries from 20 μl of each DNA extract and extraction blank control following the protocol from

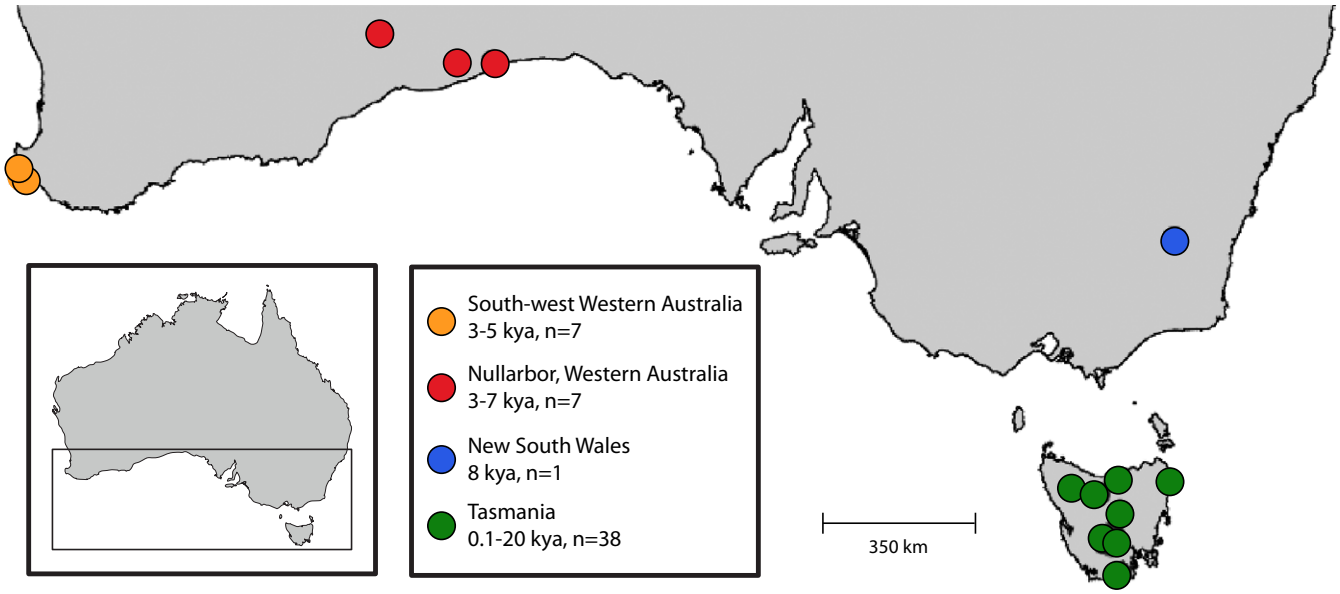

FIGURE 1 Sample locations of sequenced thylacine individuals coloured by broad geographical area. We combined some closely neighbouring localities. Seventeen of the 38 Tasmanian samples did not have locations recorded and are therefore not represented on the map [Colour figure can be viewed at wileyonlinelibrary.com]

Meyer and Kircher (2010). We used custom adapters that featured internal barcode sequences to allow multiplexing of individuals and in-silico de-multiplexing downstream. Every batch of libraries prepared included a library blank control.

Commercially synthesised biotinylated 80-mer RNA baits (MYcroarray, MI, USA) were used to enrich the target libraries for thylacine mitochondrial DNA. Baits were designed as part of the commercial service using published thylacine mitochondrial sequences from Miller et al. (2009). A second set of baits was designed to include the mitochondrial genome sequence of a mainland thylacine produced using the first set of baits. We chose to exclude the control region from the second set of baits because the large amounts of repetitive DNA in that region had resulted in low mapping quality. One round of hybridization capture was performed per the manufacturer's protocol (MYbaits, v2 manual) with modifications (see Appendix S2).

All enriched libraries were quality tested using the Tapestation 2200 (Agilent Technologies, Santa Clara, USA) and sequenced in 2 × 150 (i.e. paired-end) reactions on Illumina NextSeq and MiSeq machines at the Australian Genome Research Facility, Adelaide.

2.3 | Sequence processing and mitochondrial genome assembly

Raw reads were de-multiplexed and internal barcodes removed using sabre (https://github.com/najoshi/sabre) before being processed and mapped to a thylacine mitochondrial reference sequence (GenBank Accession: NC011944) using the PALEOMIX 1.1 pipeline (Schubert et al., 2014). Briefly, we removed adapter contamination using the default settings in ADAPTERREMOVAL 2.1 (Lindgreen, 2012) except using a minimal read length of 25 bp. Mapping was performed using BWA 0.7.7 (Li & Durbin, 2009), disabling the seed and relaxing the edit distance (option $-n = 0.01$) as suggested by Schubert et al. (2012). Separate sequencing runs of the same libraries were combined before PCR duplicates were removed using SAMTOOLS 0.1.18 (Li et al., 2009) and MARKDUPLICATES from the Picard package (http://broadinstitute.github.io/picard/). MAPDAMAGE2 (Jónsson, Ginolhac, Schubert, Johnson & Orlando, 2013), implemented in PALEOMIX, was used to demonstrate damage patterns consistent with ancient DNA template by modelling post-mortem DNA damage from patterns of nucleotide misincorporations for each library.

Finally, all alignments were visually inspected in GENEIOUS 10.0.2 and consensus sequences were called for all positions where >60% of the sequences agreed and read depth was at least three. Where there was no >60% majority, bases were called as the appropriate IUPAC ambiguity symbol. Regions with insufficient read depth were coded as N.

We aligned all consensus sequences and two publically available Tasmanian thylacine mitogenome sequences (GenBank accession: NC011944 and FJ515781; Miller et al., 2009) using MAFFT (Katoh, Misawa, Kuma & Miyata, 2002) as implemented in GENEIOUS. We chose to trim the control region from the alignment because of low coverage and poor mapping quality.

2.4 | Descriptive statistics

Descriptive statistics (haplotype diversity H_d, nucleotide diversity π, number of segregating sites S, and the average number of segregating sites between individuals k) were calculated on samples grouped by geography and temporal period using DNASP 5.1 (Librado & Rozas, 2009). The single NSW sample was excluded from this analysis because it was the sole representative of that geographical area. Undated ancient samples were also excluded, as they could not be accurately placed into a temporal period. For comparison, we

calculated the same statistics on a sample (n = 13) of contemporary devil mitochondrial genomes (Genbank accession: JX475454–JX475467; Miller, Eldridge, Morris, Zenger & Herbert, 2011; Miller, Hayes, Ratan, et al., 2011) which were modified to also exclude the control region.

DNASP was also used to test for demographic changes in the historical Tasmanian thylacine samples using Tajima's D (Tajima, 1989), and Fu and Li's estimators D^* and F^* (Fu & Li, 1993). The significance of the demographic estimators was obtained by examining the null distribution of 5,000 coalescent simulations of these statistics. Demographic estimator analysis was restricted to the historical Tasmanian samples to avoid effects of heterochrony (Depaulis, Orlando & Hänni, 2009).

To further test for evidence of population expansion in the historical Tasmanian samples we generated a pairwise mismatch distribution (Rogers & Harpending, 1992) on the data in DNASP. The number of observed differences between pairs of mitochondrial genomes was compared to the expected distribution of differences under specified demographic models (i.e. constant population size or population growth). By using τ, the mode of the observed mismatch distribution, and the mean mutation rate inferred for the Tasmanian population using BEAST (see below) we estimated the time of expansion by the relationship $t = \tau/2u$, in which t is the time of expansion and u is the cumulative (across sequence) probability of substitution. To this result we added the average age of all the historic thylacines (165 years), to calculate the time of expansion in years BP. The calculation was carried out using the online tool provided by Schenekar and Weiss (2011).

2.5 | Phylogenetic analysis

The program POPART (Leigh & Bryant, 2015) was used to construct a TCS haplotype network from the alignment of all sequenced individuals and the two publically available sequences, including samples with unknown ages (n = 53). Sites with more than 5% missing data were masked (Leigh & Bryant, 2015).

We constructed a time-scaled phylogenetic tree in BEAST 2.4.1 (Bouckaert et al., 2014) using the same alignment. We used the mean calibrated radiocarbon date and the known or estimated collection dates for historic specimens as calibration points (Bouckaert et al., 2014). When we included our ancient samples without radiocarbon/collection dates in order to estimate their ages (Shapiro et al., 2011), our BEAST analyses failed to converge. Consequently, we excluded our ancient samples with unknown ages from the final BEAST analysis (n = 44). The coalescent extended Bayesian skyline model (Heled & Drummond, 2008), with a relaxed lognormal clock, was used as it was preferred to the constant population size coalescent when tested using the modified Akaike information criterion (AICM) in TRACER 1.6 (Table S2.2, Baele et al., 2012). Despite the intra-species nature of the data, our relaxed lognormal clock analysis rejected the use of a global clock (i.e. the posterior estimates for the coefficient of variation were non-zero; Drummond & Bouckaert, 2015).

An appropriate partitioning scheme for phylogenetic analysis was determined using the program PARTITIONFINDER 1.1.1 (Lanfear, Calcott, Ho & Guindon, 2012). We used an input of 43 regions: first, second and third codon positions of each mitochondrial protein-coding gene; non-coding regions; 12s rRNA; 16s rRNA; and concatenated tRNAs (Table S2.3). The optimum partitioning scheme was chosen based on the Bayesian information criterion. The BEAST Markov chain Monte Carlo (MCMC) was run twice with different seed values for 30 million generations sampling every 1,000 generations. All parameters showed convergence and sufficient sampling in both runs (indicated by effective sampling sizes above 200) when inspected in TRACER 1.6, with the first 10% of samples discarded as burn-in (Rambaut, Suchard, Xie & Drummond, 2014). A maximum clade credibility (MCC) tree was annotated in TREEANNOTATOR 2.4.1 and visualizzed in FIGTREE 1.4.2 (Rambaut, 2007).

A date randomization test was conducted to check whether the temporal signal from the radiocarbon dates associated with ancient and historic sequences were sufficient to calibrate the analysis (Ho et al., 2011). This test randomizes all dates and determines whether the 95% high posterior density (HPD) intervals of the mean rates estimated from the date-randomized datasets include the mean rate estimated from the original dataset (Figure S2.1-2). In addition, a "leave-one-out-cross-validation" (LOOCV) test was performed to test for bias and error in the sequences and associated dates (Shapiro et al., 2011). In particular, we tested whether the assumed date of 120 yr BP was appropriate for historic samples without specific dates attached to them (Figure S2.3). Input .xml files for the date randomization and LOOCV tests were generated using the R package "TipDatingBeast" (Rieux & Khatchikian, 2016).

2.6 | Inferences of demographic history

We used the extended Bayesian skyline model implemented in BEAST 2.4.1, with prior and MCMC settings as above, to estimate the demographic history of the Tasmanian thylacine population. We restricted this analysis to the Tasmanian population as the phylogenetic analysis of the whole dataset revealed significant structure and the date randomization test showed insufficient temporal information among the WA samples alone (Figure S2.2). As above, the analysis was run twice and in both runs all parameters showed convergence and sufficient sampling, with the first 10% of samples discarded as burn-in.

We also inferred the thylacines demographic history from the dated mitochondrial sequences using Approximate Bayesian Computation (ABC) as implemented in DIYABC 2.1.0 (Cornuet et al., 2014). We tested six scenarios that represent an ancestral divergence followed by different combinations of bottlenecks and expansions in two geographically separated groups (Tasmania vs. Western Australia; Figure 2). The single NSW sample was also excluded from this analysis. The prior distributions of historical, demographic and mutational parameters are described in Table 1. We chose to use a normal distribution for the time of ancestral divergence (based on our results from BEAST), as we were most interested in the post-

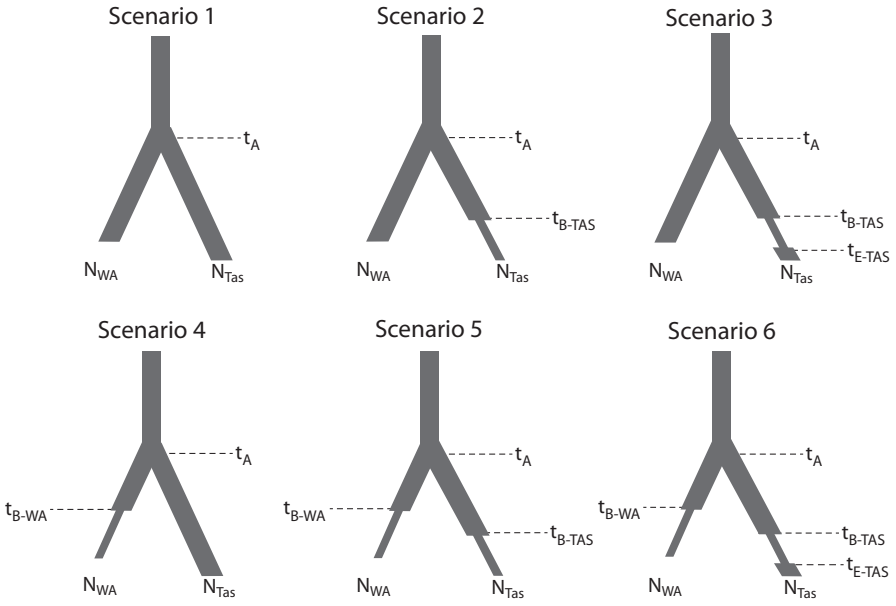

FIGURE 2 Demographic models of thylacine population history across southern Australia tested using ABC analysis. Branch widths indicate relative population size. Dashed lines indicate time of inferred population size changes

TABLE 1 Prior distributions for demographic parameters used in ABC analysis of thylacine mitochondrial genomes from samples collected from southern Australia. *Ne* is used for effective population size

Interpretation	Parameter	Distribution	Min	Max	Mean	*SD*	Conditions
Ne Tas (most recent)	N_{TAS}	Uniform	10	10,000	–	–	–
Ne WA (most recent)	N_{WA}	Uniform	10	50,000	–	–	–
Ne Tas (bottleneck)	N_{TAS1}	Uniform	10	10,000	–	–	$<N_{TAS}$
Ne Tas (post-divergence)	N_{TAS2}	Uniform	10	100,000	–	–	$>N_{TAS1}$
Ne WA (post-divergence)	N_{WA2}	Uniform	10	100,000	–	–	$>N_{WA}$
Ancestral divergence time	t_A	Normal	10,000	100,000	30,000	12,000	–
Tas expansion time	$t_{E\text{-}TAS}$	Uniform	0	20,000	–	–	$<t_{B\text{-}TAS}$
Tas bottleneck time	$t_{B\text{-}TAS}$	Uniform	0	40,000	–	–	$<t_A$
WA bottleneck time	$t_{B\text{-}WA}$	Uniform	3,200	40,000	–	–	$<t_A$
Mutation model	U	Uniform	1.00×10^{-9}	1.00×10^{-6}	–	–	HKY
Mutation model	K	Uniform	0.5	20	–	–	–

divergence demographic changes for this analysis. We chose to use a generation time of four years as this falls between that of the Tasmanian devil (*c.* 3 years), and the grey wolf (*Canis lupis*, *c.* 5 years), a species with which the thylacine shares many convergent affinities (Jones et al., 2008; Mech, Barber-Meyer & Erb, 2016; Wroe, Clausen, McHenry, Moreno & Cunningham, 2007; Wroe & Milne, 2007).

Each scenario was simulated based on neutral coalescence for 10^6 iterations and summary statistics (number of haplotypes, number of segregating sites, mean and variance of pairwise differences and F_{st}) were computed for each simulation. DIYABC draws random values for each parameter from the prior distributions and performs coalescent-based simulations to generate simulated samples with the same number of samples and loci per population as the observed dataset. A Euclidean distance is then calculated between the summary statistics of each simulated dataset and the observed dataset (Beaumont, Zhang & Balding, 2002).

The posterior probability of each scenario was estimated using logistic regression on the 1% of simulated datasets closest to the observed dataset, subject to linear discriminant analysis as a pre-processing step (Estoup et al., 2012). The selected scenario was the one with the highest posterior probability value, with the 95% confidence interval (CI) not overlapping the 95% CI of any other compared scenario. We estimated the posterior distribution of each demographic parameter under the best demographic model by carrying out local linear regression on the closest 1% of simulated datasets, after the application of logit transformation to parameter values (Cornuet et al., 2014).

3 | RESULTS

3.1 | Sequencing results

We successfully sequenced the mitochondrial genome (15,447 bp excluding the control region) from 51 thylacines (15 from the mainland and 36 from Tasmania, Figure 1). Thirty additional samples produced <1,000 unique reads or <50% coverage and were excluded

TABLE 2 Genetic diversity summary statistics calculated from thylacine and devil mitochondrial genomes from sampled collected from Tasmania (Tas) and Western Australia (WA). Number of samples (*n*), number of haplotypes (*H*), haplotype diversity (H_d), number of segregating sites (*S*), nucleotide diversity (π), average pairwise difference (*k*), Fu and Li's demographic estimators *D** and *F**, Tajima's *D* (*Td*), mode of the observed mismatch distribution (τ) and estimated time of expansion in years BP. Devil mitochondrial genomes were sourced from Miller, Eldridge, et al. (2011) and Miller, Hayes, et al. (2011): GenBank accessions JX475454–JX475467 and were modified to exclude the control region

Group	*n*	Age range	*H*	H_d	*S*	π	*k*	*D**	*F**	Td	τ	Exp. time
Tas Historic	30	96–500	10	0.862	14	0.00017	2.37	−1.39	−1.52	−1.098	1.583	736
Tas Ancient	3	8–20 ka	3	1	32	0.00138	21.333	–	–	–	–	–
WA Ancient	10	3–8 ka	9	0.978	44	0.00168	14.489	–	–	–	–	–
Tas Devils	13	0–50	8	0.897	25	0.0005	7.62	0.049	0.10123	0.1961	–	–

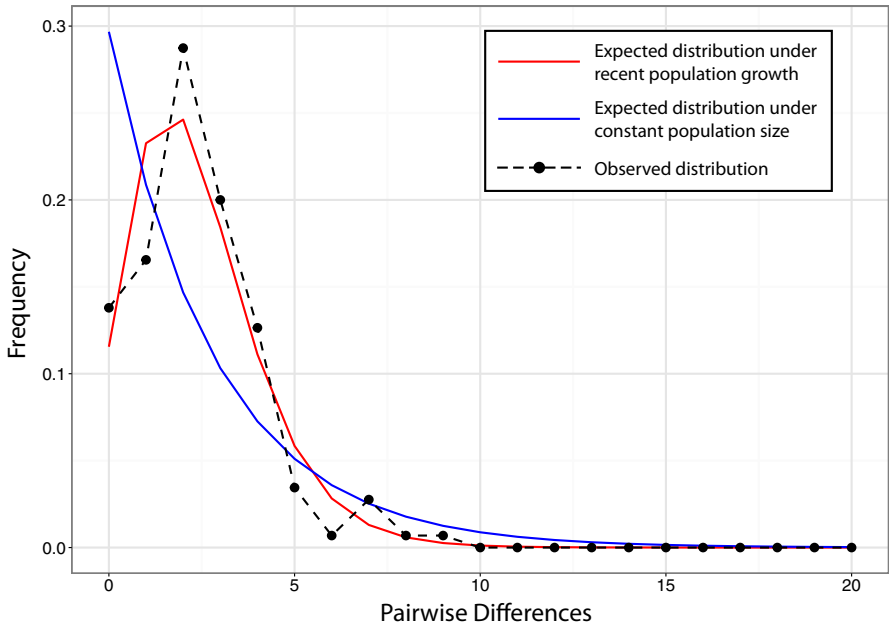

FIGURE 3 Mismatch distribution constructed from aligned historical Tasmanian thylacine mitochondrial sequences [Colour figure can be viewed at wileyonlinelibrary.com]

from further analysis. Forty-two dated samples range in age from 88 to 20,812 yr BP (Table S1.1). The average coverage and depth was high for both the ancient samples (age >600 yr BP, mean coverage = 95.8%, mean depth = 152.2) and historic samples (age <600 yr BP, mean coverage = 99.5%, mean depth = 1,177.7). Full details of sequencing and mapping statistics are available in Appendix 3 (Table S3.1). All libraries showed cytosine deamination frequencies and distributions consistent with ancient or museum specimen DNA (Figure S3.1). All library and extraction blank controls had no more than two reads that mapped to the reference sequence (Table S3.1).

3.2 | Descriptive statistics and network

Genetic diversity was lower across all measures in the historic Tasmanian thylacine population than in the ancient Tasmanian or ancient Western Australian groups (Table 2). Genetic diversity in historic Tasmanian group was also lower than in a sample of modern Tasmanian devils despite greater temporal range. The demographic estimators, Fu and Li's *D** and *F**, and Tajima's *D*, were all non-significantly negative. The shape of the pairwise mismatch distribution suggests that the historic Tasmanian thylacine population had expanded prior to their decline to extinction (Figure 3). Using τ, we estimated the timing of this expansion to be 736 yr BP.

3.3 | Phylogenetic analysis

The TCS network (Figure 4) shows two distinct groups: western thylacines versus Tasmanian and NSW thylacines. There is no structure separating the two sampling locations within the western group and the single NSW sample falls between two ancient Tasmanian samples. The undated western samples fall in with the rest of the western samples, which are genetically diverse. Three of the undated Tasmanian samples are grouped with the most frequent haplotype representing most of the historic samples. The other two undated Tasmanian samples share a haplotype with an ancient Tasmanian individual (Sample #9708) that was dated as 8,263 yr BP.

BEAST analyses estimated the average mutation rate to be 1.27×10^{-7} substitutions per site, per year. This rate falls within the range (*c.* 1×10^{-7}–10^{-8}) recently estimated for numerous ancient mitochondrial DNA datasets (Ho et al., 2011). The MCC tree (Figure 5) showed that the Tasmanian group (including the single NSW sample) and the western group diverged *c.* 30,000 yr BP (20,725–48,780 95% HPD). The most recent common ancestor

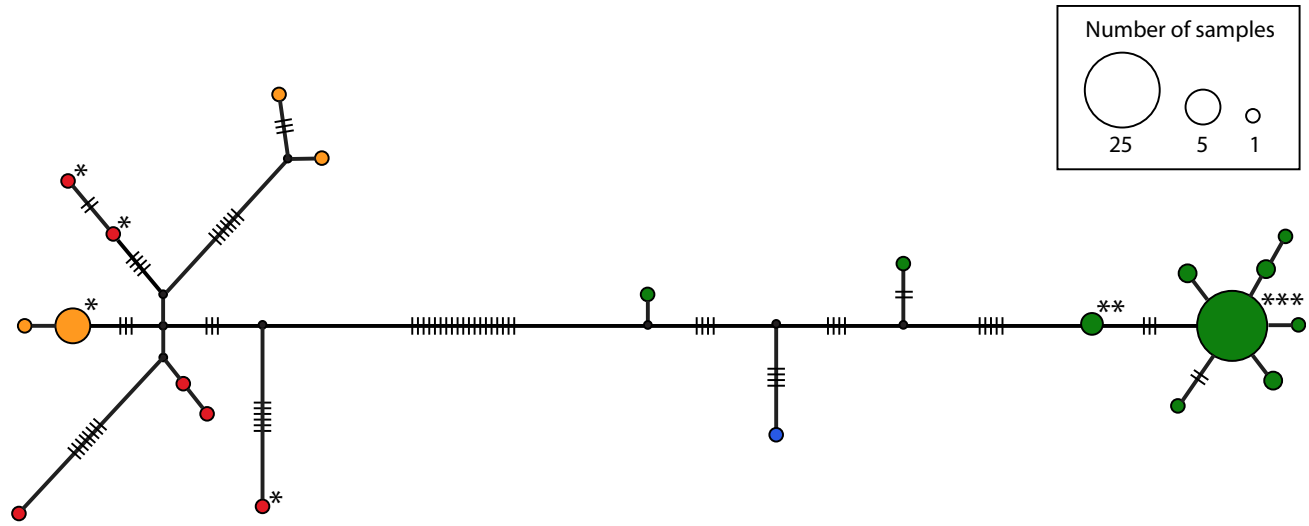

FIGURE 4 TCS network based on the alignment of 53 thylacine mitochondrial genome sequences (15,447 bp). Circle size is proportional to the frequency of haplotypes. Hatch marks represent the number of mutations between haplotypes. Black dots represent unsampled haplotypes and other colours relate to geographical location as presented in Figure 1 (orange = south-west WA, red = Nullarbor, WA, blue = NSW and green = Tasmania). Asterisks show the position of the nine undated ancient samples. The network was built with sites with >5% missing data masked meaning that the number of haplotypes and mutations are underrepresented [Colour figure can be viewed at wileyonlinelibrary.com]

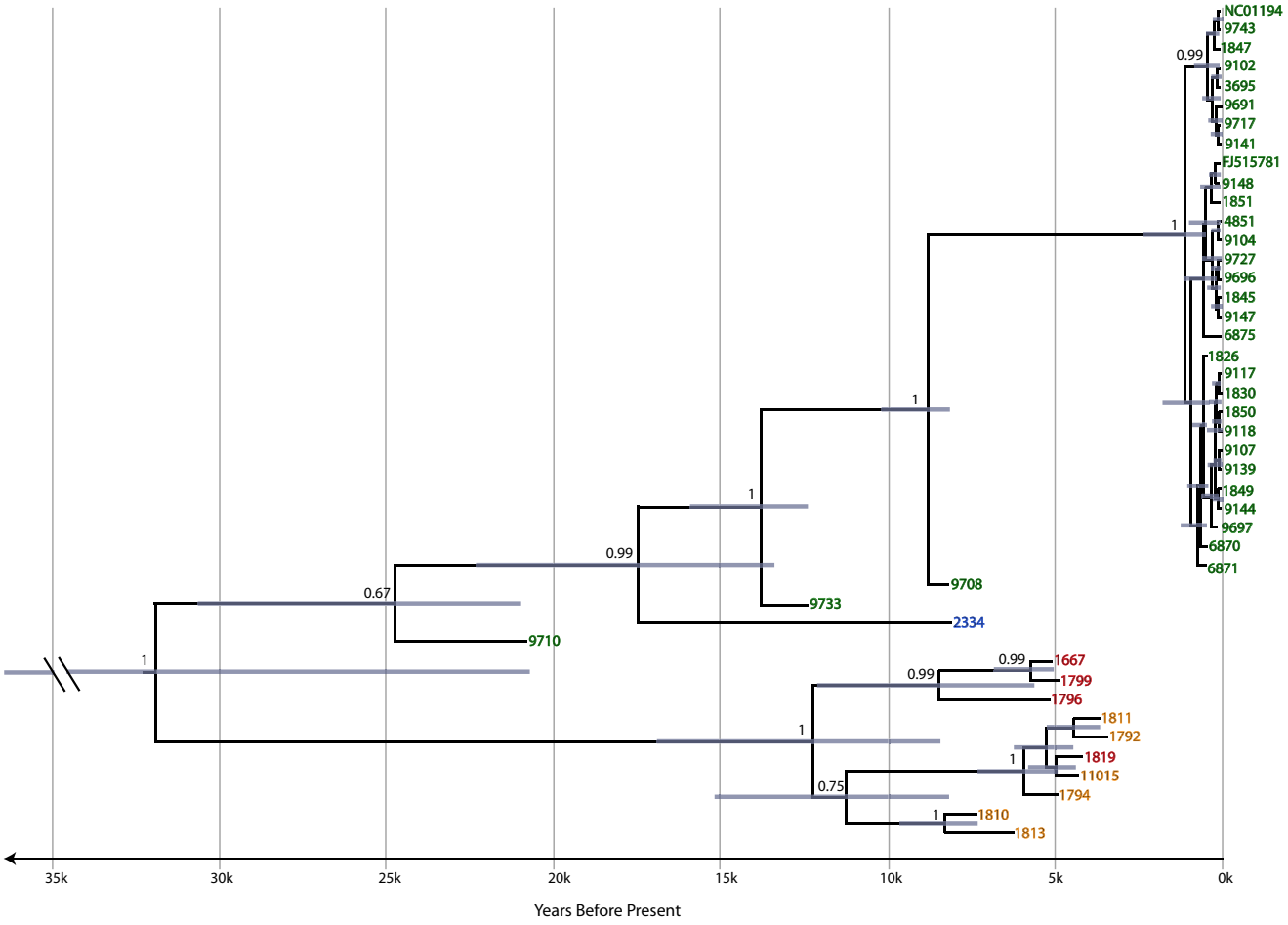

FIGURE 5 BEAST maximum clade credibility phylogeny of thylacine mitochondrial sequences for which radiocarbon dates were available. Nodes are labelled with Bayesian posterior probabilities (PP) for nodes with PP >0.5. Node height reflects mean posterior age. Grey bars at nodes represent the 95% HPD of node age. Double slanted lines indicate that a portion of the bar has been omitted because of space constraints. Colours correspond to geographical location as shown in Figure 1 [Colour figure can be viewed at wileyonlinelibrary.com]

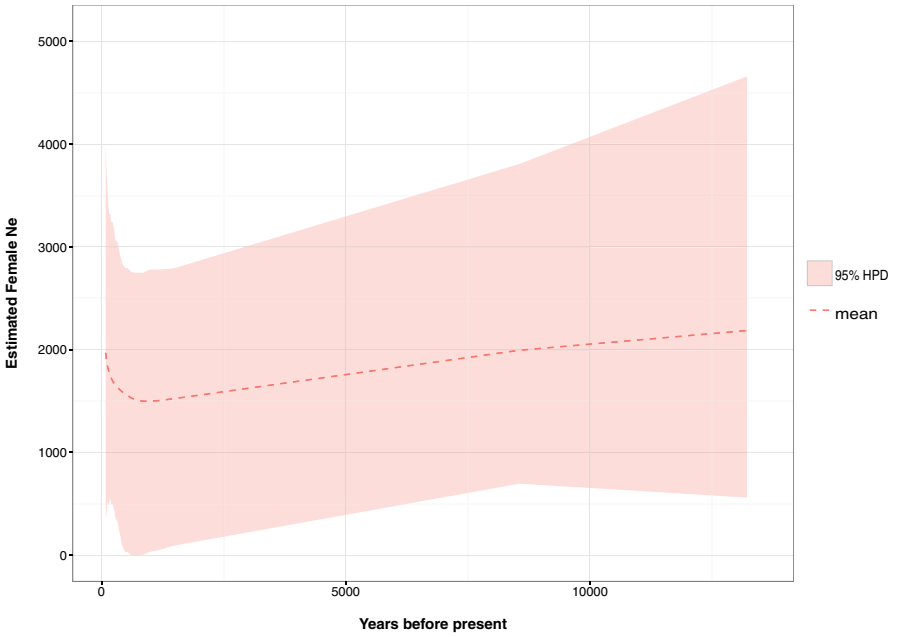

FIGURE 6 Extended Bayesian skyline plot of female effective population size in the Tasmanian thylacine population [Colour figure can be viewed at wileyonlinelibrary.com]

(TMRCA) was *c.* 12,000 yr BP (8,449–16,813 95% HPD) for the western group, *c.* 25,000 yr BP (20,959–30,535 95% HPD) for the eastern group including the ancient samples, and *c.* 1,000 yr BP (455–2293 95% HPD) for the historic Tasmanian samples. The single NSW sample falls within the ancient Tasmanian samples.

3.4 | Inference of demographic history

The coalescent-based Bayesian skyline plot shows a slow and slight decline over the last *c.* 15,000 years, followed by an expansion in the Tasmanian population beginning *c.* 1,000 yr BP (Figure 6). However, confidence intervals are wide and a constant population size through time cannot be rejected.

ABC analysis identified Scenario 3 as the most likely scenario (Table S3.2). In Scenario 3 the population size of the western group remained constant and the Tasmanian group expanded after a bottleneck (Figure 7). The estimated parameters under Scenario 3 are given in Table 3. The timing of bottleneck and recovery in Tasmania are estimated to be 20,400 (6,440–36,520 95% CI) and 3,160 (192.8–16,960 95% CI) year BP respectively. We note that the generation time estimate used (4 years) may deviate from the thylacines true generation time, possibly biasing the timing of inferred events. However, our ABC time estimates are broadly consistent with the demography inferred by our Bayesian skyline analysis.

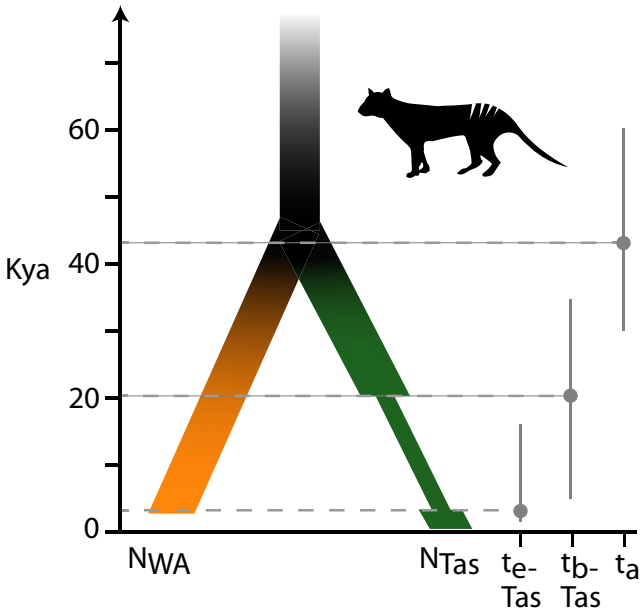

FIGURE 7 The thylacine demographic scenario selected by ABC analysis (Scenario 3). Time is given in thousands of years before present (ka). Time estimates are provided as the median and 95% confidence intervals (grey dots and error bars). The width of the branches represents relative population size [Colour figure can be viewed at wileyonlinelibrary.com]

4 | DISCUSSION

Our analyses of thylacine mtDNA revealed an east-west phylogeographical split, higher genetic diversity and effective population size in western versus Tasmanian populations, and evidence for a late Pleistocene or Holocene population bottleneck and recent population expansion in the Tasmanian population.

4.1 | Phylogenetic patterns in mainland thylacines

The divergence between the two groups seen in our phylogenetic analysis is suggestive of isolation by distance or a demographic scenario in which the thylacines retracted into western and eastern refugia around the time of the Last Glacial Maximum (LGM, *c.* 25,000 yr BP). Evidence for retraction into east/west refugia during the LGM has been observed in a range of Australian birds

TABLE 3 Posterior distributions of parameters from the selected scenario (Scenario 3) from ABC analysis of thylacine mitochondrial genomes from samples collected from southern Australia

Parameter	Median	q05	q95	Mean	Mode
N_{TAS}	4,470	1,440	9,320	4,850	3,510
N_{WA}	15,600	4,350	42,400	18,500	6,920
N_{TAS1}	787	77.2	3,270	1,110	67.3
N_{TAS2}	55,500	10,200	96,000	54,500	96,300
t_A	42,400	28,160	60,000	42,800	39,280
$t_{E\text{-}TAS}$	3,160	192.8	16,960	5,400	116
$t_{B\text{-}TAS}$	20,400	6,440	36,520	20,880	19,880
u	2.61×10^{-7}	1.18×10^{-7}	5.12×10^{-7}	2.81×10^{-7}	2.61×10^{-7}
k	9.48	0.9	18.8	9.62	1.64

(Dolman & Joseph, 2012; Murphy, Joseph, Burbidge & Austin, 2011) and mammals (Cooper, Bertozzi, Baynes & Teale, 2003; Miller, Eldridge, et al., 2011; Miller, Hayes, et al., 2011). The same pattern of east/west divergence has been suggested for mainland devils based on fossil occurrences, but is not observed in the fossil distribution of mainland thylacines, possibly due to taphonomic bias (Brown, 2006; Owen, 2003). The Nullarbor and/or Lake Eyre regions are well-characterized biogeographical barriers for many terrestrial vertebrates and may have obstructed gene flow between populations during and after the LGM, a pattern that is evident in numerous extant vertebrate fauna (Austin, Joseph, Pedler & Black, 2013; Byrne et al., 2008; Marin et al., 2013; Neaves, Zenger, Prince & Eldridge, 2013). Several thylacine samples used in our study are from the Nullarbor with ages ranging from 3–7 thousand years, indicating that the western group was present on the Nullarbor immediately preceding the groups extinction. Thus, we suggest the Eyrean barrier (Lake Eyre/Flinders Ranges) as a more likely barrier for thylacines.

This apparent structuring may also be due to isolation by distance, given that eastern Australia is represented by a single mainland sample, and several mammals show evidence of Late Pleistocene range expansion across the Nullarbor and Eyrean barriers. For example, the red kangaroo (*Macropus rufus*), western grey kangaroo (*Macropus fuliginosus*), western pygmy possum (*Cercartetus concinnus*) and fat tailed dunnart (*Sminthopsis crassicaudata*) have wide distributions with limited genetic structure across southern Australia (Clegg, Hale & Moritz, 1998; Cooper, Adams & Labrinidis, 2000; Neaves, Zenger, Prince & Eldridge, 2012; Pestell, Cooper, Saint & Petit, 2007). Increased sampling in the east and, crucially, in southern and south-eastern Australia, will be needed to confirm whether our results show retracting populations or simply isolation by distance across the species range.

The single NSW sample falls within the eastern group, bracketed by older and younger ancient Tasmanian samples, indicating that Tasmanian and mainland populations were connected via the Bass Strait land bridge before it was flooded for a final time *c.* 14,000 yr BP (Lambeck & Chappell, 2001). The Bass Strait land bridge has acted both as a barrier and a corridor for different terrestrial vertebrates. Koalas (*Phascolarctos cinereus*) never crossed the land bridge to reach Tasmania, whilst several mammals (e.g. Frankham, Handasyde & Eldridge, 2016; Gongora et al., 2012), frogs (e.g. Symula, Keogh & Cannatella, 2008) and reptiles (e.g. Dubey & Shine, 2010) show deep (>0.9 Myr, Pliocene/Pleistocene) divergences, suggesting ancient vicariance with no subsequent dispersal. In contrast, several other reptiles (Chapple, Keogh & Hutchinson, 2005) and frogs (Schäuble & Moritz, 2001) crossed the land bridge in the late Pleistocene to colonize Tasmania from Victoria. More samples are needed from eastern Australia to reconstruct demographic history of thylacines in this region and to establish the extent of gene flow between Tasmania and the mainland during the late Pleistocene.

The estimated female effective population size and genetic diversity of the western population was much larger than the Tasmanian population. We do not detect any genetic patterns of decline in the Western Australian population prior to their extinction approximately 3,200 yr BP. This could indicate that, like the Tasmanian thylacines, the mainland thylacine decline to extinction was rapid and not the result of intrinsic factors, such as inbreeding depression.

4.2 | Tasmanian thylacine demographic history

Our data suggest that the Tasmanian thylacine population was increasing prior to European arrival. ABC analysis indicates that this expansion represents a recovery from a population bottleneck. The 95% CI surrounding the estimated time of this bottleneck is large (6,440–36,520 yr BP), possibly because ABC analysis restricts demographic scenarios to abrupt events. In contrast, the Bayesian skyline plot of the Tasmanian population suggests that the decline may have been slow and incremental, feasibly the result of the isolation of Tasmania from the mainland. However, the CI surrounding the estimated size change is also large. While mitochondrial DNA has many properties useful for genetic analysis and can be easier to retrieve from degraded specimens, future studies should focus on multiple nuclear loci to gain more precise estimates of demographic history of the thylacines (Heled & Drummond, 2008; Ho & Gilbert, 2010).

Regardless of the mode of decline, the low genetic diversity in the Tasmanian thylacine population reveals that their effective population size was small. ABC inference suggests that the effective female population size was fewer than 1,000 individuals (median = 787, 95% CI 77.2–3270) prior to the expansion, increasing to 4,470 (95% CI 1,440–9,320) in historic times. We do not detect any genetic patterns of population decline leading up to the extinction of thylacines in 1936, likely because the extirpation occurred so quickly (Owen, 2003).

4.3 | Comparison with Tasmanian devils

The demographic history of thylacines and devils show a number of striking parallels that contrast with other terrestrial carnivores with similar distributions. Both species were widespread on the mainland during the Pleistocene but became extinct there at the same time (approximately 3,200 yr BP) and both species survived a population bottleneck (or, in the thylacine's case, at least long-term low *Ne* due to island insularity), resulting in low genetic diversity in Tasmania (Brüniche-Olsen et al., 2014). In contrast, tiger quolls and eastern quolls (the next largest marsupial carnivores in Tasmania and eastern Australia) did not go extinct on the mainland and have higher levels of genetic diversity (Firestone, Elphinstone, Sherwin & Houlden, 1999). This suggests that an ecological crisis severely impacted thylacines and devils, sometime in the mid- to late-Holocene, but did not affect other marsupial carnivores. Habitat preferences (quolls favour wetter forest, while thylacines and devils were more abundant in drier, open sclerophyll forest) may explain the contrasting response (Jones & Barmuta, 2000; Jones & Stoddart, 1998).

We cannot support or refute the hypothesis that thylacines underwent an abrupt bottleneck at the same time as devils, but we suggest that our results do support an environmental change in Tasmania at that time. The overall similarity in demographic histories suggests that a regime shift in the broad Tasmanian ecosystem caused population declines in both species. Given the absence of other drivers evident in Tasmania at the time, Brüniche-Olsen et al. (2014) propose the intensification of the ENSO climate system as the driver of the devils late-Holocene decline. During the late-Holocene, ENSO associated events resulted in greater variability in rainfall and increased duration and intensity of droughts across Australia (Donders et al., 2008). Although this climate variability is assumed to have been less pronounced in Tasmania than on the mainland (Donders et al., 2007), several studies of palaeoecological proxies have linked vegetation changes and fire events on the island to ENSO activity (Beck, Fletcher, Gadd, Heijnis & Jacobsen, 2017; Fletcher et al., 2014; Stahle, Whitlock & Haberle, 2016).

Unstable climate, changes in vegetation states and altered fire regimes have been linked to changes in vertebrate population dynamics on the Australian mainland and other continents (Dortch, 2004; Hadly, 1996; Jaksic, Silva, Meserve & Gutiérrez, 1997; Lima, Stenseth & Jaksic, 2002; Marshal, Owen-Smith, Whyte & Stenseth, 2011). To test for a relationship between ENSO-linked environmental change and population size changes in the Tasmanian thylacine and devils, a greater understanding of prey abundances in Tasmania during the late-Holocene is needed.

4.4 | Implications for the devil and thylacine mainland extinctions

It has been assumed that ENSO activity had minimal impact on Tasmania. However, our results and other recent studies show that climate change may have impacted the top marsupial predators on the island. Given that climate change impacts are known to have been more severe on the mainland, this could indicate that ENSO activities have been underestimated as a potential driver of the devil and thylacine's mainland extinctions. Alternatively, the contrasting outcomes of mainland extinction and island survival may suggest that climate change alone was insufficient to cause the mainland extinctions. This is congruent with a recent simulation study that identified synergistic effects of climate change and human intensification as a probable cause of the thylacine and devil mainland extinctions (Prowse et al., 2013).

4.5 | Summary

Using the largest dataset of thylacine DNA sequences to date we provide the first genetic evidence that mainland thylacines split into eastern and western remnant populations in southern Australia prior to the LGM and show that the ancient western population had a larger effective population size than the recent Tasmanian population. We find no evidence for a loss of genetic diversity leading to the extinction of the western population, indicating that the mainland extinction was rapid and not the result of intrinsic factors, such as inbreeding depression.

We showed that, like devils, Tasmanian thylacines had relatively low genetic diversity, the result of a bottleneck event or island insularity. However, unlike Tasmanian devils, our analyses suggest that the Tasmanian thylacine population was expanding prior to European arrival. The timing of this expansion, in concert with a decline in Tasmanian devils and an ENSO-associated climate event, points to a possible environmental regime shift in Tasmania *c.* 3,000 yr BP. Given that ENSO effects are known to have been more severe on mainland Australia, we suggest that climate change, in synergy with other drivers (such as human intensification or dingo competition/predation), is likely to have contributed to the devil and thylacine mainland extinction.

To gain further understanding of the thylacine's demographic history and processes that led to their extinction, future studies should focus on multiple nuclear loci and strive for increased sampling in south-central and eastern mainland Australia. The Fossahul database (https://doi.org/10.4227/05/564e6209c4fe8) of dated Australian fossils lists 32 thylacine fossils from south-central (i.e. South Australia and Victoria) and 27 from eastern (i.e. NSW and Queensland) mainland Australia (Rodríguez-Rey et al., 2016). While this list does not include undated material and many of the listed fossils are of an age outside the range from which it would be possible to retrieve DNA, the database shows the plausibility of filling in our sampling gaps in the future.

Climate projections predict a hotter and more arid climate across Australia in coming decades, which will exacerbate and add to existing threats to native species (CSIRO and Bureau of Meteorology, 2015). Therefore, understanding the impact of past climate change on Australian native fauna and disentangling its effects from that of human pressure and invasive species is critical for understanding extinction risk and focusing conservation efforts in the future.

ACKNOWLEDGEMENTS

We thank the Western Australian Museum, Queen Victoria Museum and Art Gallery, South Australian Museum, Museum Victoria, Australian National Wildlife Collection (CSIRO), Tasmanian Museum and Art Gallery, American Museum of Natural History, Oxford Museum of Natural History, Leeds Museum, Swedish Museum of Natural History and M. Bunce (Curtin University) for granting permission to sample thylacine specimens. We also thank S. Donnellan and three anonymous reviewers for helpful comments on the manuscript. This research was supported by ARC Future Fellowship (FT10010008) and Discovery Project (DP130104055) grants to J.J.A.

DATA ACCESSIBILITY

All DNA sequence data are deposited in GenBank accession numbers: KY678342–KY678392.

ORCID

Lauren C. White http://orcid.org/0000-0001-8085-9293

REFERENCES

Austin, J. J., Joseph, L., Pedler, L. P., & Black, A. B. (2013). Uncovering cryptic evolutionary diversity in extant and extinct populations of the southern Australian arid zone Western and Thick-billed Grasswrens (Passeriformes: Maluridae: *Amytornis*). *Conservation Genetics*, *14*, 1173–1184.

Baele, G., Lerney, P., Bedford, T., Rambaut, A., Suchard, A., & Alekseyenka, A. V. (2012). Improving the accuracy of demographic and molecular clock model comparison while accommodating phylogenetic uncertainty. *Molecular Biology and Evolution*, *9*, 2157–2167.

Beaumont, M. A., Zhang, W., & Balding, D. J. (2002). Approximate Bayesian computation in population genetics. *Genetics*, *162*, 2025–2035.

Beck, K. K., Fletcher, M.-S., Gadd, P. S., Heijnis, H., & Jacobsen, G. E. (2017). An early onset of ENSO influence in the extra-tropics of the southwest Pacific inferred from a 14, 600 year high resolution multiproxy record from Paddy's Lake, northwest Tasmania. *Quaternary Science Reviews*, *157*, 164–175.

Bouckaert, R., Heled, J., Kühnert, D., Vaughan, T., Wu, C.-H., Xie, D., … Drummond, A. J. (2014). BEAST 2: A software platform for Bayesian evolutionary analysis. *PLoS Computational Biology*, *10*, e1003537.

Brotherton, P., Haak, W., Templeton, J., Brandt, G., Soubrier, J., Adler, C. J., … The Genographic Consortium. (2013). Neolithic mitochondrial haplogroup H genomes and the genetic origins of Europeans. *Nature Communications*, *4*, 1764.

Brown, O. J. F. (2006). Tasmanian devil (*Sarcophilus harrisii*) extinction on the Australian mainland in the mid-Holocene: Multicausality and ENSO intensification. *Alcheringa An Australasian Journal of Palaeontology*, *30*, 49–57.

Brüniche-Olsen, A., Jones, M. E., Austin, J. J., Burridge, C. P., & Holland, B. R. (2014). Extensive population decline in the Tasmanian devil predates European settlement and devil facial tumour disease. *Biology Letters*, *10*, 20140619.

Byrne, M., Yeates, D. K., Joseph, L., Kearney, M., Bowler, J., Williams, M. A. J., … Wyrwoll, K.-H. (2008). Birth of a biome: Insights into the assembly and maintenance of the Australian arid zone biota. *Molecular Ecology*, *17*, 4398–4417.

Chapple, D. G., Keogh, J. S., & Hutchinson, M. N. (2005). Substantial genetic substructuring in southeastern and alpine Australia revealed by molecular phylogeography of the *Egernia whitii* (Lacertilia: Scincidae) species group. *Molecular Ecology*, *14*, 1279–1292.

Clegg, S. M., Hale, P., & Moritz, C. (1998). Molecular population genetics of the red kangaroo (*Macropus rufus*): mtDNA variation. *Molecular Ecology*, *7*, 679–686.

Cooper, S. J. B., Adams, M., & Labrinidis, A. (2000). Phylogeography of the Australian dunnart *Sminthopsis crassicaudata* (Marsupialia: Dasyuridae). *Australian Journal of Zoology*, *48*, 461–473.

Cooper, N. K., Bertozzi, T., Baynes, A., & Teale, R. J. (2003). The relationship between eastern and western populations of the heath rat, *Pseudomus shortridgei* (Rodentia: Muridae). *Records - Western Australian Museum*, *21*, 367–370.

Corbett, L. K. (1995). *The dingo in Australia and Asia*. Ithaca, New York: Cornell University Press.

Cornuet, J.-M., Pudlo, P., Veyssier, J., Dehne-Garcia, A., Gautier, M., Leblois, R., … Estoup, A. (2014). DIYABC v2.0: A software to make approximate Bayesian computation inferences about population history using single nucleotide polymorphism, DNA sequence and microsatellite data. *Bioinformatics*, *30*, 1187–1189.

CSIRO and Bureau of Meteorology. (2015). *Climate Change in Australia Information for Australia's Natural Resource Management Regions: Technical Report*. Australia: CSIRO and Bureau of Meteorology.

Depaulis, F., Orlando, L., & Hänni, C. (2009). Using classical population genetics tools with heterochroneous data: Time matters!. *PLoS ONE*, *4*, e5541.

Dolman, G., & Joseph, L. (2012). A species assemblage approach to comparative phylogeography of birds in southern Australia. *Ecology and Evolution*, *2*, 354–369.

Donders, T. H., Haberle, S. G., Hope, G., Wagner, F., & Visscher, H. (2007). Pollen evidence for the transition of the Eastern Australian climate system from the post-glacial to the present-day ENSO mode. *Quaternary Science Reviews*, *26*, 1621–2637.

Donders, T. H., Wagner-Cremer, F., & Visscher, H. (2008). Integration of proxy data and model scenarios for the mid-Holocene onset of modern ENSO variability. *Quaternary Science Reviews*, *27*, 571–579.

Dortch, J. (2004). Late Quaternary vegetation change and the extinction of black-flanked rock-wallaby (*Petrogale lateralis*) at Tunnel Cave, southwestern Australia. *Palaeogeography, Palaeoclimatology, Palaeoecology*, *211*, 185–204.

Drummond, A. J., & Bouckaert, R. R. (2015). *Bayesian evolutionary analysis with BEAST*. Cambridge, UK: Cambridge University Press.

Dubey, S., & Shine, R. (2010). Evolutionary diversification of the lizard genus *Bassiana* (Scincidae) across southern Australia. *PLoS ONE*, *5*, e12982.

Estoup, A., Lombaert, E., Marin, J.-M., Guillemaud, T., Pudlo, P., Robert, C. P., & Cornuet, J.-M. (2012). Estimation of demo-genetic model probabilities with approximate Bayesian computation using linear discriminant analysis on summary statistics. *Molecular Ecology Resources*, *12*, 846–855.

Firestone, K. B., Elphinstone, M. S., Sherwin, W. B., & Houlden, B. A. (1999). Phylogeographical population structure of tiger quolls *Dasyurus maculatus* (Dasyuridae: Marsupialia), an endangered carnivorous marsupial. *Molecular Ecology*, *8*, 1613–1625.

Fletcher, M.-S., Wolfe, B. B., Whitlock, C., Pompeani, D. P., Heijnis, H., Haberle, S. G., … Bowman, D. M. J. S. (2014). The legacy of mid-Holocene fire on a Tasmanian montane landscape. *Journal of Biogeography*, *41*, 476–488.

Frankham, G. J., Handasyde, K. A., & Eldridge, M. D. B. (2016). Evolutionary and contemporary responses to habitat fragmentation

detected in a mesic zone marsupial, the long-nosed potoroo (Potorous tridactylus) in south-eastern Australia. *Journal of Biogeography*, *4*, 653–665.

Fu, Y. X., & Li, W. H. (1993). Statistical tests of neutrality of mutations. *Genetics*, *133*, 693–709.

Gongora, J., Swan, A. B., Chong, A. Y., Ho, S. Y. W., Damayanti, C. S., Kolomyjec, S., … Gust, N. (2012). Genetic structure and phylogeography of platypuses revealed by mitochondrial DNA. *Journal of Zoology*, *286*, 110–119.

Hadly, E. A. (1996). Influence of late-Holocene climate on northern Rocky Mountain mammals. *Quaternary Research*, *46*, 298–310.

Harris, G. P. (1808). XI Description of two new species of Didelphis from Van Dieman's Land. *Transactions of the Linnean Soceity of London*, *9*, 174–178.

Heled, J., & Drummond, A. J. (2008). Bayesian inference of population size history from multiple loci. *BMC Evolutionary Biology*, *8*, 289.

Ho, S. Y. W., & Gilbert, M. T. P. (2010). Ancient mitogenomics. *Mitochondrion*, *10*, 1–11.

Ho, S. Y. W., Lanfear, R., Phillips, M. J., Barnes, I., Thomas, J. A., Kolokotronis, S.-O., & Shapiro, B. (2011). Bayesian estimation of substitution rates from ancient DNA sequences with low information content. *Systematic Biology*, *60*, 366–375.

Jaksic, F. M., Silva, S. I., Meserve, P. L., & Gutiérrez, J. R. (1997). A long-term study of vertebrate predator responses to an El Niño (ENSO) disturbance in Western South America. *Oikos*, *78*, 341–354.

Johnson, C. (2006). *Australia's mammal extinctions: A 50,000-year history*. Port Melbourne, Australia: Cambridge University Press.

Johnson, C. N., & Wroe, S. (2003). Causes of extinction of vertebrates during the Holocene of mainland Australia: Arrival of the dingo, or human impact? *Holocene*, *13*, 941.

Jones, M. E., & Barmuta, L. A. (2000). Niche differentiation among sympatric Australian dasyurid carnivores. *Journal of Mammalogy*, *81*, 434–447.

Jones, M. E., Cockburn, A., Hamede, R., Hawkins, C., Hesterman, H., Lachish, S., … Pemberton, D. (2008). Life-history change in disease-ravaged Tasmanian devil populations. *Proceedings of National Academy of Sciences*, *105*, 10023–10027.

Jones, M. E., Paetkau, D., Geffen, E., & Moritz, C. (2004). Genetic diversity and population structure of Tasmanian devils, the largest marsupial carnivore. *Molecular Ecology*, *13*, 2197–2209.

Jones, M. E., & Stoddart, D. M. (1998). Reconstruction of the predatory behaviour of the extinct marsupial thylacine (*Thylacinus cynocephalus*). *Journal of Zoology*, *246*, 239–246.

Jónsson, H., Ginolhac, A., Schubert, M., Johnson, P. L., & Orlando, L. (2013). mapDamage2. 0: Fast approximate Bayesian estimates of ancient DNA damage parameters. *Bioinformatics*, *29*, 1682–1684.

Katoh, K., Misawa, K., Kuma, K., & Miyata, T. (2002). MAFFT: A novel method for rapid multiple sequence alignment based on fast Fourier transform. *Nucleic Acids Research*, *30*, 3059–3066.

Lambeck, K., & Chappell, J. (2001). Sea level change through the last glacial cycle. *Science*, *292*, 679–686.

Lanfear, R., Calcott, B., Ho, S. Y. W., & Guindon, S. (2012). PartitionFinder: Combined selection of partitioning schemes and substitution models for phylogenetic analyses. *Molecular Biology and Evolution*, *29*, 1695–1701.

Leigh, J. W., & Bryant, D. (2015). Popart: Full-feature software for haplotype network construction. *Methods in Ecology and Evolution*, *6*, 1110–1116.

Li, H., & Durbin, R. (2009). Fast and accurate short read alignment with Burrows-Wheeler transform. *Bioinformatics*, *25*, 1754–1760.

Li, H., Handsaker, B., Wysoker, A., Fennell, T., Ruan, J., Homer, N., … Durbin, R.; 1000 Genome Project Data Processing Subgroup (2009). The sequence alignment/map format and SAMtools. *Bioinformatics*, *25*, 2078–2079.

Librado, P., & Rozas, J. (2009). DnaSP v5: A software for comprehensive analysis of DNA polymorphism data. *Bioinformatics*, *25*, 1451–1452.

Lima, M., Stenseth, N. C., & Jaksic, F. M. (2002). Food web structure and climate effects on the dynamics of small mammals and owls in semi-arid Chile. *Ecology Letters*, *5*, 273–284.

Lindgreen, S. (2012). AdapterRemoval: Easy cleaning of next generation sequencing reads. *BMC Research Notes*, *5*, 337.

Marin, J., Donnellan, S. C., Hedges, S. B., Puillandre, N., Aplin, K. P., Doughty, P., … Vidal, N. (2013). Hidden species diversity of Australian burrowing snakes (*Ramphotyphlops*). *Biological Journal of the Linnean Society*, *110*, 427–441.

Marshal, J. P., Owen-Smith, N., Whyte, I. J., & Stenseth, N. C. (2011). The role of El Niño-Southern Oscillation in the dynamics of a savanna large herbivore population. *Oikos*, *120*, 1175–1182.

Mech, L. D., Barber-Meyer, S. M., & Erb, J. (2016). Wolf (*Canis lupus*) generation time and proportion of current breeding females by age. *PLoS ONE*, *11*, e0156682.

Menzies, B. R., Renfree, M. B., Heider, T., Mayer, F., Hildebrandt, T. B., & Pask, A. J. (2012). Limited genetic diversity preceded extinction of the Tasmanian tiger. *PLoS ONE*, *7*, e35433.

Meyer, M., & Kircher, M. (2010). Illumina sequencing library preparation for highly multiplexed target capture and sequencing. *Cold Spring Harbor Protocols*, *2010*, doi:10.1101/pdb.prot5448.

Miller, W., Drautz, D. I., Janecka, J. E., Lesk, A. M., Ratan, A., Tomsho, L. P., … Schuster, S. C. (2009). The mitochondrial genome sequence of the Tasmanian tiger (*Thylacinus cynocephalus*). *Genome Research*, *19*, 213–220.

Miller, E. J., Eldridge, M. D. B., Morris, K. D., Zenger, K. R., & Herbert, C. A. (2011). Genetic consequences of isolation: Island tammar wallaby (*Macropus eugenii*) populations and the conservation of threatened species. *Conservation Genetics*, *12*, 1619–1631.

Miller, W., Hayes, V. M., Ratan, A., et al. (2011). Genetic diversity and population structure of the endangered marsupial *Sarcophilus harrisii* (Tasmanian devil). *Proceedings of the National Academy of Sciences*, *108*, 12348–12353.

Murphy, S. A., Joseph, L., Burbidge, A. H., & Austin, J. (2011). A cryptic and critically endangered species revealed by mitochondrial DNA analyses: The western ground parrot. *Conservation Genetics*, *12*, 595–600.

Neaves, L. E., Zenger, K. R., Prince, R. I. T., & Eldridge, M. D. B. (2012). Impact of Pleistocene aridity oscillations on the population history of a widespread, vagile Australian mammal, *Macropus fuliginosus*. *Journal of Biogeography*, *39*, 1545–1563.

Neaves, L. E., Zenger, K. R., Prince, R. I. T., & Eldridge, M. D. B. (2013). Paternally inherited genetic markers reveal new insights into genetic structuring within *Macropus fuliginosus* and hybridisation with sympatric *Macropus giganteus*. *Australian Journal of Zoology*, *61*, 58–68.

Owen, D. (2003). *Thylacine: The tragic tale of the Tasmanian tiger*. Crows Nest, NSW: Allen and Unwin.

Pestell, A. J. L., Cooper, S. J. B., Saint, K., & Petit, S. (2007). Genetic structure of the western pygmy possum, *Cercartetus concinnus*, Gould (Marsupialia: Burramyidae) based on mitochondrial DNA. *Australian Mammalogy*, *29*, 191–200.

Prowse, T. A. A., Johnson, C. N., Bradshaw, C. J. A., & Brook, B. W. (2013). An ecological regime shift resulting from disrupted predator-prey interactions in Holocene Australia. *Ecology*, *95*, 693–702.

Rambaut, A. (2007). FigTree, a graphical viewer of phylogenetic trees. Retrieved from: http://tree.bio.ed.ac.uk/software/figtree. Accessed date: December 2016

Rambaut, A., Suchard, M. A., Xie, D., & Drummond, A. J. (2014). Tracer v1.6. Retrieved from http://beast.bio.ed.ac.uk/Tracer.

Rees, A. B. H., Cwynar, L. C., & Fletcher, M.-S. (2015). Southern Westerly Winds submit to the ENSO regime: A multiproxy paleohydrology record from Lake Dobson, Tasmania. *Quaternary Science Reviews*, *126*, 254–263.

Rieux, A., & Khatchikian, C. E. (2016). TIPDATINGBEAST: An R package to assist the implementation of phylogenetic tip-dating tests using beast. *Molecular Ecology Resources*, *17*, 608–613.

Rodríguez-Rey, M., Herrando-Pérez, S., Brook, B. W., Saltré, F., Alroy, J., Beeton, N., … Bradshaw, C. J. A. (2016). A comprehensive database of quality-rated fossil ages for Sahul's Quaternary vertebrates. *Scientific Data*, *3*, 160053.

Rogers, A. R., & Harpending, H. (1992). Population growth makes waves in the distribution of pairwise genetic differences. *Molecular Biology and Evolution*, *9*, 552–569.

Schäuble, C. S., & Moritz, C. (2001). Comparative phylogeography of two open forest frogs from eastern Australia. *Biological Journal of the Linnean Society*, *74*, 157–170.

Schenekar, T., & Weiss, S. (2011). High rate of calculation errors in mismatch distribution analysis results in numerous false inferences of biological importance. *Heredity*, *107*, 511–512.

Schubert, M., Ermini, L., Sarkissian, C. D., Jónsson, H., Ginolhac, A., Schaefer, R., … Orlando, L. (2014). Characterization of ancient and modern genomes by SNP detection and phylogenomic and metagenomic analysis using PALEOMIX. *Nature Protocols*, *9*, 1056–1082.

Schubert, M., Ginolhac, A., Lindgreen, S., Thompson, J. F., AL-Rasheid, K. A., Willerslev, E., … Orlando, L. (2012). Improving ancient DNA read mapping against modern reference genomes. *BMC Genomics*, *13*, 178.

Shapiro, B., Ho, S. Y. W., Drummond, A. J., Suchard, M. A., Pybus, O. G., & Rambaut, A. (2011). A Bayesian phylogenetic method to estimate unknown sequence ages. *Molecular Biology and Evolution*, *28*, 879–887.

Stahle, L. N., Whitlock, C., & Haberle, S. G. (2016). A 17,000-year-long record of vegetation and fire from Cradle Mountain National Park, Tasmania. *Frontier in Ecology and Evolution*, *4:82*, 1–17.

Symula, R., Keogh, J. S., & Cannatella, D. C. (2008). Ancient phylogeographic divergence in southeastern Australia among populations of the widespread common froglet, *Crinia signifera*. *Molecular Phylogenetics and Evolution*, *47*, 569–580.

Tajima, F. (1989). Statistical method for testing the neutral mutation hypothesis by DNA polymorphism. *Genetics*, *123*, 585–595.

Wroe, S., Clausen, P., McHenry, C., Moreno, K., & Cunningham, E. (2007). Computer simulation of feeding behaviour in the thylacine and dingo as a novel test for convergence and niche overlap. *Proceedings of the Royal Society of London B: Biological Sciences*, *274*, 2819–2828.

Wroe, S., & Milne, N. (2007). Convergence and remarkably consistent constraint in the evolution of carnivore skull shape. *Evolution*, *61*, 1251–1260.

BIOSKETCHES

Lauren C. White is currently a post-doctoral researcher at the Max Planck Institute for Evolutionary Anthropology. Her research there focuses on using genomic data to study kinship structure in social primate species. Her PhD thesis, completed at the University of Adelaide, focused on conservation and population genetics of Australian mammals.

Kieren J. Mitchell is interested in using ancient DNA from extinct populations and species to better understand evolutionary processes. This includes exploring how ancestral diversity is differentially inherited by daughter populations/species, inferring rates of evolution, and identifying how populations/species have reacted to past environmental change.

Jeremy J. Austin uses ancient DNA techniques through space and time to understand the evolutionary history of living and extinct mammals, reptiles and birds, to assess the impacts of past environmental change, and to provide valuable genetic data for conservation and management of threatened species.

Author contributions: L.C.W. acquired and analysed the data and drafted the manuscript; K.J.M. helped analyse the data and helped revise the manuscript; J.J.A. designed the study, collected samples, interpreted the results and helped revise the manuscript. All authors gave final approval for publication.

SUPPORTING INFORMATION

Additional Supporting Information may be found online in the supporting information tab for this article.

How to cite this article: White LC, Mitchell KJ, Austin JJ. Ancient mitochondrial genomes reveal the demographic history and phylogeography of the extinct, enigmatic thylacine (*Thylacinus cynocephalus*). *J Biogeogr*. 2018;45:1–13. https://doi.org/10.1111/jbi.13101